Experimental investigation of soft kite performance during turning maneuvers

Oehler, Johannes; Marc, Van Reijen; Schmehl, Roland

DOI
10.1088/1742-6596/1037/5/052004

Publication date
2018

Document Version
Final published version

Published in
Journal of Physics: Conference Series

Journal of Physics: Conference Series

PAPER • **OPEN ACCESS**

Experimental investigation of soft kite performance during turning maneuvers

To cite this article: Johannes Oehler *et al* 2018 *J. Phys.: Conf. Ser.* **1037** 052004

IOP Conf. Series: Journal of Physics: Conf. Series **1037** (2018) 052004 doi:10.1088/1742-6596/1037/5/052004

Experimental investigation of soft kite performance during turning maneuvers

Johannes Oehler[†], **Marc van Reijen**[†‡] **and Roland Schmehl**[†]

† Delft University of Technology, the Netherlands
‡ Kitepower B.V.

E-mail: j.d.oehler@tudelft.nl

Abstract. Airborne wind energy is an evolving renewable energy technology with the potential to reduce material as well as energy investments and to harvest wind resources that have so far not been accessible. Ground generation systems use the pulling force of a kite to generate a linear traction motion driving a drum connected to a generator. To understand and quantify the aerodynamic performance of a soft kite we developed a sensor system that measures the relative flow conditions on a flying, highly flexible wing. Together with ground-based measurements of traction force, the aerodynamic efficiency of the kite can be computed. The experimental data can be used for the validation of currently available kite models.
The lift-to-drag ratio is mainly affected by the power setting or trim of the kite and the steering commands. For the first time the effect of the trim control on the kite's steering capability was quantified for a leading edge inflatable kite. We found that a trim position with higher power ratio which results in a higher angle of attack increases the steering agility of the kite. The attained yaw rate increased by 40%. For optimization of future power kites it is important to understand the mechanisms affecting a kite's performance.

1. Introduction

The geometrical dimensions of full-scale flexible wing kites for airborne wind energy systems (AWES) generally prohibit measurements in the controlled environment of a typical wind tunnel. Down-scaling is challenging because the deformation of the structure must be scaled as well which makes model building very complicated. Fluid-structure interaction tools are being developed but not available yet for a full three dimensional analysis of a flexible kite. This is why several attempts have been undertaken to measure the aerodynamics of a flexible wing kite in real size flight experiments. Stevenson [1] used a moving platform as well as a kite flying on a circular trajectory to determine its performance. Hummel [2] developed a towing test setup achieving good repeatability. However, major shortcomings of these tests are:

- Traction force is limited because of the characteristics of the test platform.
- Atmospheric wind variations induce a significant uncertainty on calculated lift coefficients.
- Using ground-based measurements only, the lift-to-drag ratio L/D cannot be obtained for dynamic maneuvers, further tether sag induces additional uncertainty [3].

The onboard measurement setup which is integrated into a pumping kite power system addresses all three problems. Static and dynamic flight situations can be evaluated and measurements are independent of ground station and tether. It follows Hummel's main suggestion of measuring flow magnitude and direction on the kite.

2. Experimental setup

The 20 kW AWES jointly operated by Delft University of Technology and the startup company Kitepower B.V. is illustrated schematically in Fig. 1. It is equipped with sensors on the ground station ① and on the kite ② which are used for flight control. The relative flow is measured in the bridle line system of the kite (see Fig. 1 left).

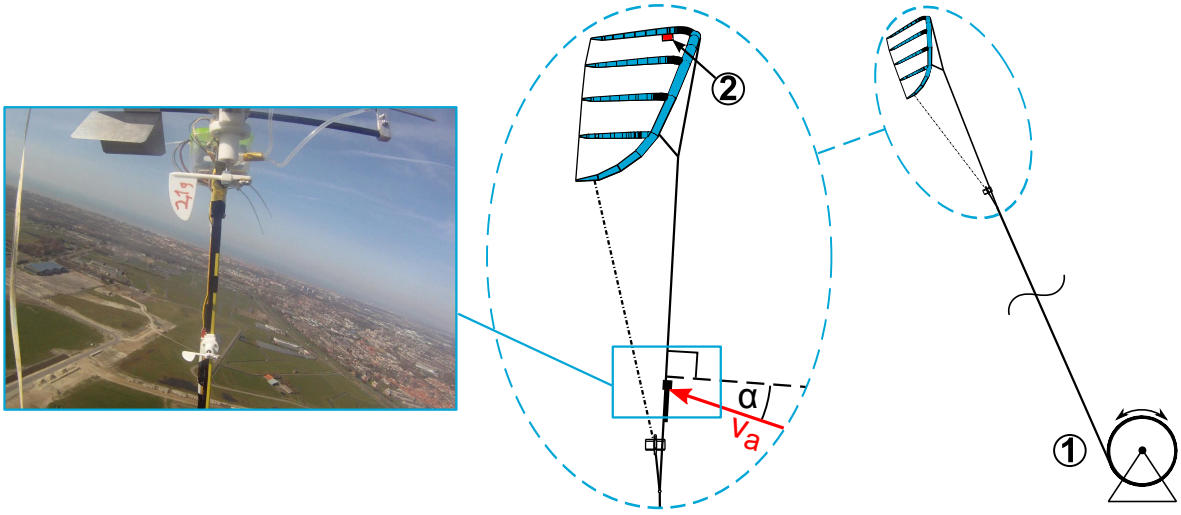

Figure 1. Experimental setup A: The AWES prototype with sensor positions.

The positioning of the flow sensor in the bridle lines limits the flow perturbation by the kite and the suspended kite control unit (KCU) that the sensor experiences. Apparent flow velocity and inflow angles are measured at all different operational conditions. The sensor uses a Pitot tube with a differential pressure sensor and angular vanes with a total magnetic encoder [4,5]. The kite employed in the test is a 25 m^2 leading edge inflatable (LEI) kite developed by the research group of TU Delft in 2012.

The second experimental setup consists of a Hydra V5 LEI surf kite, operated with fixed tether length at a low altitude. It is equipped with the same sensors, measuring angle of attack α and apparent flow speed v_a. The sensors are mounted in the kite's longitudinal axis in an air data boom configuration with a boom pointing forward in direction of flight (see Fig. 2). The

Figure 2. Experimental setup B: Hydra V5 kite with air data boom in the lab and in flight [6].

orientation of the kite is tracked by an inertial measurement unit mounted on the kite's center chord. The second setup was used to investigate the steering performance. Determining the

aerodynamic efficiency L/D was not attempted in these flights. For both experiments the data acquisition rate is $f = 20$ Hz.

3. Methodology

3.1. Lift-to-drag ratio

The quasi-steady force equilibrium of the airborne system, represented by a point mass, and the kinematic properties are illustrated schematically in Fig. 3. Based on the depicted relationships

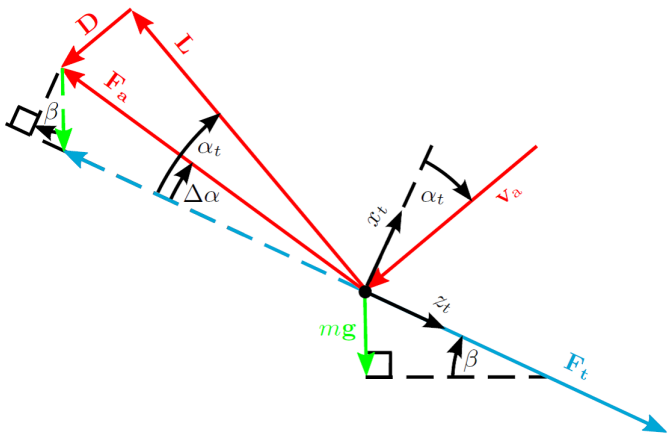

Figure 3. Relation of aerodynamic lift-to-drag ratio L/D to tether angle α_t.

the lift to drag ratio L/D can be derived as

$$\frac{L}{D} = \tan\left(\alpha_t - \Delta\alpha\right), \tag{1}$$

where α_t is the angle between the apparent flow velocity vector $\mathbf{v}_a$ and the perpendicular to the last segment of the tether (z_t in Fig. 3). This method is described in detail in [7].

The angle α_t is the sum of α which is directly obtained from the measurement and λ_0. λ_0 is the angle between the power lines where the sensor is mounted (Fig. 1) and the last tether segment z_t. This angle depends on tether force F_t, heading angle χ, geometry and weight of the airborne system and is calculated for every time step at the same frequency as the measurements of $f = 20$ Hz.

$$\alpha_t = \alpha + \lambda_0 \tag{2}$$

Since the sensor is mounted on the airborne system the measurement is independent of tether length and sag. To account for the influence of weight, $\Delta\alpha$ is introduced. The heading angle χ affects the relation between the angle α_t and the aerodynamic lift-to-drag ratio L/D through $\Delta\alpha$.

$$\Delta\alpha = \tan^{-1}\left(\frac{mg\cos(\beta)\cos(\chi)}{F_t + (mg\sin(\beta))}\right) \tag{3}$$

3.2. Turn rate law

The turn rate law establishes a relation between steering input δ and the turning of the kite. It was introduced and validated in experiments with a ram air kite by [8].

$$\dot{\psi} = G v_a \delta \tag{4}$$

In the experiments they determined the kite specific parameter G but did not propose a mechanistic model. [9] and [10] found that the same formula was applicable to leading edge inflatable kites and proposed

$$G = \frac{2C_{L,tip}}{b^2 C_{D,tip}} a \tag{5}$$

for G. a is a kite specific parameter that linearly relates tip deflection to the steering input.

Fagiano [11] linked the steering input δ to the velocity angle or course rate $\dot{\gamma}$. They used the centripetal force F_{pet} required to force the kite on its curved trajectory to derive their course rate law

$$\dot{\gamma} = \frac{F_{pet}}{m v_\tau} \tag{6}$$

The centripetal force itself is linearly related to the lift force and the steering input δ.

Fagiano assumes a small, negligible angle of sideslip β_s. Direct measurements of the sideslip angle show that its magnitude is below ten degrees in all flight operations [5]. This requires the course rate $\dot{\gamma}$ to be equal to the kite's yaw rate $\dot{\psi}$. If they differ, the sideslip angle would have to change which only happens when a turn is initiated, the turn rate is changed or at the end of a turn when the transition to straight flight happens again. Thus whenever the steering setting is constant, the sideslip angle β_s stays constant and yaw rate and course rate of the kite are equal

$$\frac{d\delta}{dt} = 0 \Rightarrow \dot{\gamma} = \dot{\psi} \tag{7}$$

This is a less severe restriction than assuming zero sideslip angle and course and heading being always equal as in [11]. Gravity has no effect on the rotation of the kite around its yaw axis, but might affect the course angle. As the aerodynamic forces are more than ten times bigger than the kite's weight we neglect gravity influence in this study as in [8]. This linear relation alone is usually referred to as the turn rate law and is supported by all published experimental data, however there is no common sense on the mechanism that leads to it. Only [11] presents a mechanistic relation to explain the turn rate parameter that changes the course angle (Eq. 6). For the yaw rate mechanism there has been a suggestions from [10] (Eq. 5).

Both [8] and [11] assume a roll maneuver, tilting the aerodynamic force vector which acts as a centripetal force that makes the kite turn. ([6,10,12]) assume a yaw maneuver of the kite which increases the lift force at one of both tips to act as centripetal force to turn the kite. The deformation of the kite makes this rotation and angle of sideslip possible [12]. Since both approaches for the turn rate of the kite, starting with centripetal force or starting with the yaw mechanism yield a linear relation between the steering input δ and the turning of the kite there is often no clear distinction ([8,11]). If (Eq. 7) holds we can conclude that both the kite's ability to yaw fast and to produce enough centripetal force are vital to its ability to corner more swiftly.

4. Results

4.1. Lift-to-drag ratio

In experiment A the kite operates at its maximal power ratio $u_p = 1$ during reel-out. The steering lines connecting the KCU to the kite's trailing edge are short with the goal of obtaining high values for both L/D and C_L. The glide ratio of the kite lies at $(L/D)_{reel-out} = 4.4$ in this case. From Fig. 4 it is apparent that a lower power ratio has a direct influence on L/D. During retraction phase where low aerodynamic performance is desired, the value drops to $(L/D)_{reel-in} = 3.2$. The experimental data quantifies the effect of depowering in a real flight scenario with power production. During the traction phase the lift-to-drag ratio occasionally drops to values below 4. The analysis shows that this coincides with strong turning maneuvers which require considerable steering inputs. These occur for example at $t = 2595$ s, $t = 2720$s

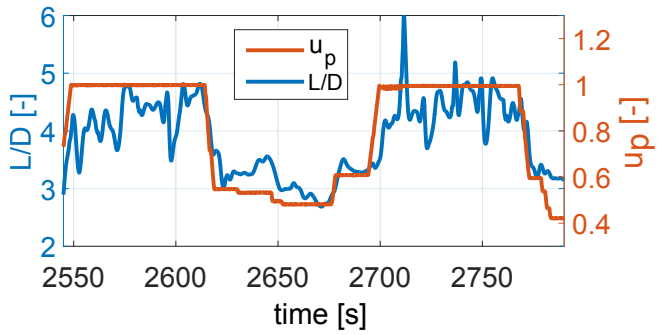

Figure 4. Variation of lift-to-drag ratio L/D with the power ratio u_p.

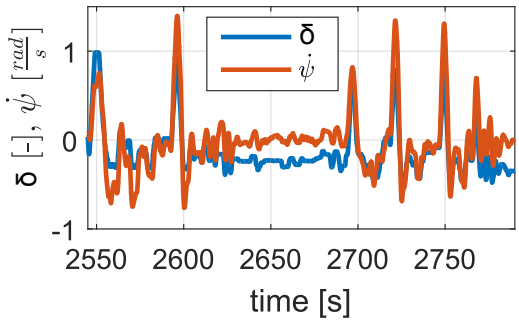

Figure 5. Influence of steering input δ on yaw rate $\dot{\psi}$.

and $t = 2750$ s and are plotted in Fig. 5. It is also apparent that the data of the steering input δ and yaw rate $\dot{\psi}$ are strongly correlated. The deformation of the kite due to the steering line deflection or the kite's rotation can be the root cause for this sharp decrease in aerodynamic performance.

4.2. Turn rate law

As can be seen in Fig. 4, there are two different power settings or trim settings used in the experimental setup A. During reel-in the power setting is low at around $u_p \in [0.4; 0.6]$, in order to realize small lift forces and a low power consumption. For reel-out the power setting is at its maximum $u_p = 1$ to produce a high lift force for high power production. This difference has a recognizable effect on the turn rate parameter G. In Fig. 6 the turn rate $\dot{\psi}$ is plotted over the product of apparent flow velocity v_a and steering input δ. During reel-in the mean value of the turn rate parameter is $G_{reel-in} = 7.3$, during reel-out it is $G_{reel-out} = 12.6$. In the plot this is visible in the steeper slope of the linear regression line for reel-out. Just as in [8] the values of the constant G are given without dimensions, its value depends on the definition of δ in (Eq. 4).

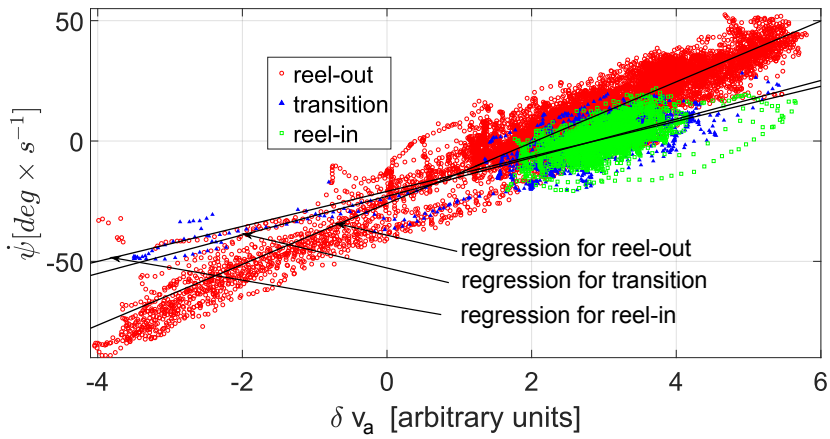

Figure 6. Turn rate of an AWES-kite during pumping cycle operation.

It is apparent from the figure that the linear trend is much clearer during reel-out. There are two reasons for that. During reel-out the kite performs active turns to follow a figure eight pattern whereas during reel-in the kite is only steered to correct for gusts and keep the kite

facing into the wind. Flying figures requires much stronger steering commands than maintaining position so we can see a much bigger range of turn rates and steering commands during reel-out. Further does the slack in the steering lines at a lower power setting result in a slower response of the kite to a steering input. As the kite is not highly loaded its shape is not very constrained and it does not always immediately respond to turning maneuvers. This behavior can also be observed during the steering experiments with the Hydra kite in the measurement campaign B. A dependency of G on the power setting u_p and thus the aerodynamic efficiency was already suggested in [9].

To get more insight into the relation of the kite's power setting to the steering capability the tests of experiment B with the Hydra V5 kite were performed with 4 different power settings. As both kites are very different in size and bridling system the power settings can not be easily related. For the Hydra kite the power settings are numbered from zero to three (see Table 1), with zero being the lowest power setting. There are two different steering maneuvers performed for each power setting. One gentle steering maneuver where the difference in line length is only few centimeters and a second one with a stronger steering input δ. They result in two distinct point clouds in each of the four plots of Fig. 7. Each of the eight maneuvers has been performed 10 times or more.

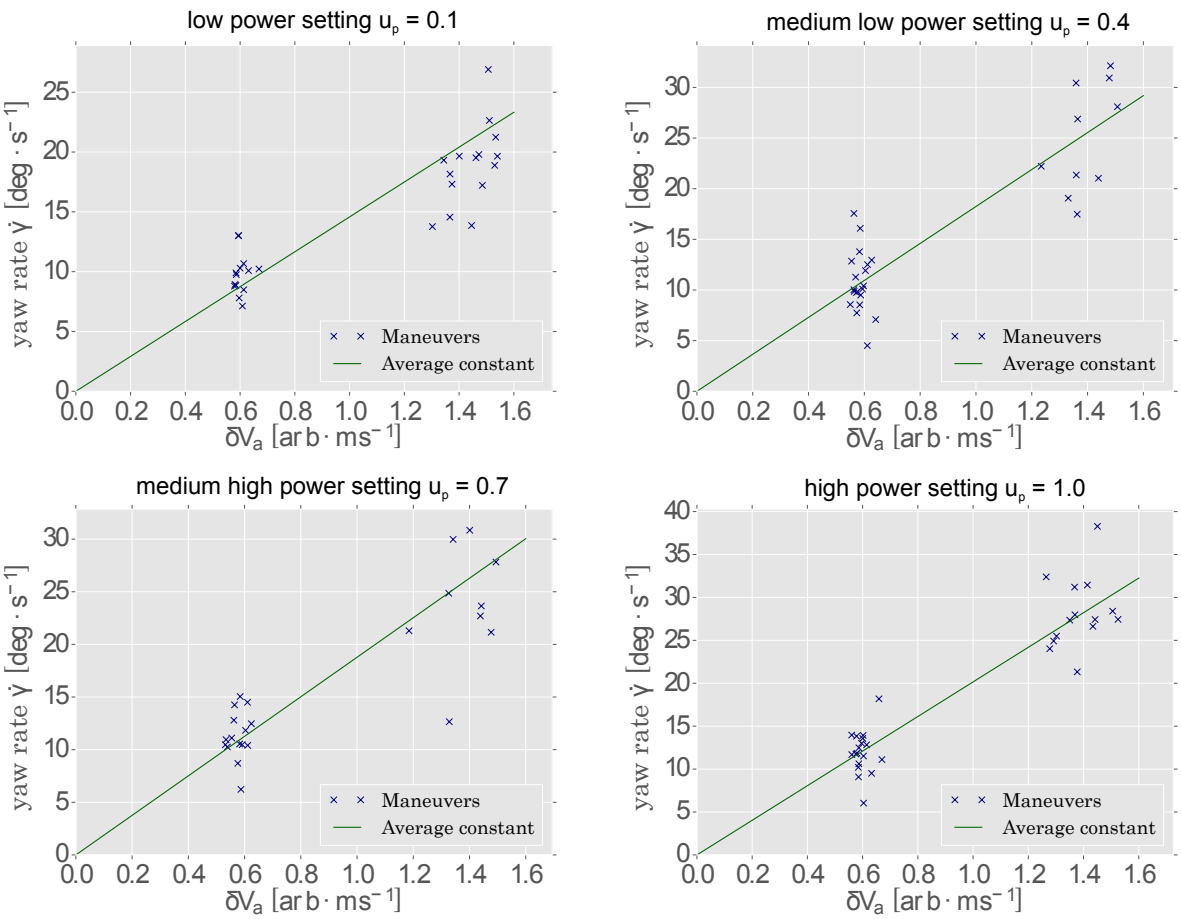

Figure 7. Turn rate experiments with different power settings for the Hydra kite [6].

The experiments support the turn rate law, suggesting a linear relation between steering input δ and the yaw rate $\dot{\psi}$. It is also visible that the higher the power setting is, the faster

Table 1. Values of the turn rate parameter G for different power settings.

Experiment	A	A	A	B	B	B	B
power setting u_p	$u_p < 0.6$	$0.6 < u_p < 0.95$	$u_p = 1$	0.1	0.4	0.7	1.0
turn rate parameter G	7.3	8.0	12.6	14.3	17.8	18.7	20.1

the kite will turn. To point out this finding from both experiments the turn rate parameter G is shown in table 1 together with the corresponding power setting. Since the two experiments use different kites and a different notation of the steering signal δ the values of G should not be directly compared.

The turn rate parameter G increases in the same way as the lift-to-drag ratio L/D with the power setting u_p in both experiments as it is suggested in (Eq. 5). It seems possible to develop and validate a more mechanistic model for the turning behavior of kites, however this must include a study with many more kites and a methodology that renders the experiments more comparable. Both this study with Table 1 and (Eq. 5) as well as [11] suggest that the turning capability increases linearly with the lift coefficient C_L and decreases for a bigger span b of the kite.

5. Conclusion and Outlook

With the help of an in-situ measurement on the airborne device the behavior of a power kite can be studied during dynamic flight maneuvers. The lift-to-drag ratio can be calculated for traction and retraction phase. The active pitching and steering mechanisms are found to have a substantial effect on its value. To realize good turning performance the kite must both yaw fast and produce a high centripetal force. Turning maneuvers decrease the lift-to-drag ratio, adversely the lower aerodynamic efficiency of a depowered kite decreases turning efficiency. Increasing a kite's power setting was found to make it turn 30% to 40% faster with respect to a low power setting. Changing power setting corresponds to a change in trim, so we can conclude that the so-called 'turn rate constant' is only a constant parameter if we do not change the trim of the kite.

The sideslip angle during a turn could be used as an indication whether the yawing or the course rate change of a kite is more effective. In an ideal case, turns without sideslip angle might be possible. Further studies should include a more precise tracking of the deformation and turning mechanism and how it affects the aerodynamic performance of the kite. Only after understanding the influence of kite shape and deformation its design can be optimized for aerodynamic performance.

Acknowledgments

The authors acknowledge the support of the team of Kitepower B.V. in flying the measurement setup on their prototype and all team members who helped us with the Hydra kite experiments. This project has received funding from the European Union's Horizon 2020 research and innovation programme under the Marie Skłodowska-Curie grant agreement No. 642682 for the ITN project AWESCO and the grant agreement No. 691173 for the "Fast Track to Innovation" project REACH.

References

[1] Stevenson J C 2003 Traction Kite Testing and Aerodynamics. PhD thesis, University of Canterbury. `https://ir.canterbury.ac.nz/bitstream/handle/10092/7688/stevenson_thesis.pdf`

[2] Hummel J 2017 Automatisierte Vermessung und Charakterisierung der dynamischen Eigenschaften seilgebundener, vollflexibler Tragflaechen. PhD thesis, TU Berlin
[3] Python B 2017 Methodology Improvement for Performance Assessment of Pumping Kite Power Wing. Master thesis, Ecole polytechnique federale de Lausanne
[4] Oehler J 2017 Measuring Apparent Flow Vector on a Flexible Wing Kite. Master thesis, University of Stuttgart
[5] Oehler J and Schmehl R 2017 Experimental Characterization of a Force-Controlled Flexible Wing Traction Kite. *Proc. Airborne Wind Energy Conf.* Freiburg, Germany `http://awec2017.com/images/posters/Poster_Oehler.pdf`
[6] van Reijen M 2018 The turning of kites. Master thesis, Delft University of Technology `resolver.tudelft.nl/uuid:5836c754-68d3-477a-be32-8e1878f85eac`
[7] Oehler J and Schmehl R 2018 Measuring aerodynamic efficiency of a soft kite through direct flow measurement. Submitted to Wind Energy Science
[8] Erhard M and Strauch H 2013 Control of towing kites for seagoing vessels *IEEE Trans. Control Syst. Technol.* **21** No.5 DOI 10.1109/TCST.2012.2221093.
[9] Jehle C 2012 Automatic Flight Control of Tethered Kites for Power Generation. Master thesis, Technical University of Munich `https://mediatum.ub.tum.de/?id=1185997`
[10] Ruppert M 2012 Development and validation of a real time pumping kite model. Master thesis, Delft University of Technology
[11] Fagiano L, Zgraggen A U, Morari M and Khammash M 2014 Automatic Crosswind Flight of Tethered Wings for Airborne Wind Energy: Modeling, Control Design and Experimental Results *IEEE Trans. Control Syst. Technol.* **22** No.4 DOI: 10.1109/TCST.2013.2279592
[12] Breukels J 2011 An Engineering Methodology for Kite Design. PhD thesis, Delft University of Technology ISBN 9789088912306 `http://resolver.tudelft.nl/uuid:cdece38a-1f13-47cc-b277-ed64fdda7cdf`